TITLE PAGE

Full-length title:

Sequential appearance and isolation of a SARS-CoV-2 recombinant between two major SARS-CoV-2 variants in a chronically infected immunocompromised patient

Short title (for the running head):

SARS-CoV-2 recombinations between variants during chronic infection

Author list: Emilie BUREL[1,2 ¥], Philippe COLSON[1,2,3 ¥], Jean-Christophe LAGIER[1,2,3], Anthony LEVASSEUR[1,2], Marielle BEDOTTO[1], Philippe LAVRARD[1,2,3], Pierre-Edouard FOURNIER[1,2,4], Bernard LA SCOLA[1,2,3 *], Didier RAOULT[1,2 *]

Affiliations: [1] IHU Méditerranée Infection, 19-21 boulevard Jean Moulin, 13005 Marseille, France; [2] Aix-Marseille Univ., Institut de Recherche pour le Développement (IRD), Microbes Evolution Phylogeny and Infections (MEPHI), 27 boulevard Jean Moulin, 13005 Marseille, France; [3] Assistance Publique-Hôpitaux de Marseille (AP-HM), 264 rue Saint-Pierre, 13005 Marseille, France; [4] Aix-Marseille Univ., Institut de Recherche pour le Développement (IRD), Vecteurs – Infections Tropicales et Méditerranéennes (VITROME), 27 boulevard Jean Moulin, 13005 Marseille, France.

[¥] Contributed equally

*** Corresponding author:** Didier Raoult, IHU Méditerranée Infection, 19-21 boulevard Jean Moulin, 13005 Marseille, France. Tel.: +33 413 732 401, Fax: +33 413 732 402; email: didier.raoult@gmail.com; Bernard La Scola, IHU Méditerranée Infection, 19-21 boulevard Jean Moulin, 13005 Marseille, France. Tel.: +33 413 732 401, Fax: +33 413 732 402; email: bernard.la-scola@univ-amu.fr.

Key words: SARS-CoV-2; variant; recombination; chronic infection; immunosuppression

Word counts: abstract, 212; text, 2,353

Figures: 3; **Tables:** 2; **References:** 48; **Supplementary Material:** Supplementary Methods, Results, Figure S1, and Table S1.

ABSTRACT

Genetic recombination is a major evolutionary mechanism among RNA viruses, and it is common in coronaviruses, including those infecting humans. A few SARS-CoV-2 recombinants have been reported to date whose genome harbored combinations of mutations from different mutants or variants, but a single patient's sample was analyzed, and the virus was not isolated. Here, we re-port the gradual creation of a hybrid genome of B.1.160 and Alpha variants in a lymphoma patient chronically infected for 14 months, and we isolated the recombinant virus. The hybrid genome was obtained by next-generation sequencing, and recombination sites were confirmed by PCR. This consisted of a parental B.1.160 backbone interspersed with two fragments, including the spike gene, from an Alpha variant. Analysis of seven sequential samples from the patient decoded the recombination steps, including the initial infection with a B.1.160 variant, then a concurrent infec-tion with this variant and an Alpha variant, the generation of hybrid genomes, and eventually the emergence of a predominant recombinant virus isolated at the end of the patient’s follow-up. This case exemplifies the recombination process of SARS-CoV-2 in real life, and it calls for intensifying genomic surveillance in patients coinfected with different SARS-CoV-2 variants, and more gener-ally with several RNA viruses, as this may lead to the creation of new viruses.

TEXT

INTRODUCTION

A major evolutionary mechanism of RNA viruses is genetic recombination [1,2]. Recombinations are extremely common in coronaviruses and have been implicated in the emergence of several genotypes, including endemic human coronaviruses [3-6]. The involvement of genetic recombination in the origin of SARS-CoV-2 is also suspected [7]. Regarding SARS-CoV-2, coinfection in the same patient with distinct variants has been reported [8-14]. In addition, several studies have described or suspected genetic recombinations for this virus [10,13-14,15-25]. However, most of these recombinants relied solely on the coexistence of signature mutations of different SARS-CoV-2 variants in ge-nomes obtained from a single patient's sample, and they were not isolated in culture. Since January 2020, our laboratory has screened more than one million respiratory specimens for SARS-CoV-2 infection by real-time reverse transcription-PCR (qPCR) without interruption or limited capacity including for all patients sampled in our institute and in the Marseille public hospitals [26,27]. This has provided us with sequential samples from multiple patients, and enabled us to detect reinfections, and prolonged or even chronic infections in severely immunocompromised patients [28-30]. Here, we re-port the gradual creation of a recombinant SARS-CoV-2 involving two variants in a lymphoma patient chronically infected over a period of 14 months, and the isolation of the recombinant virus in culture.

RESULTS

Chronic SARS-CoV-2-infection in a severely immunocompromised patient

An immunocompromised adult patient had an uncontrolled SARS-CoV-2 infection for 14 months until death (Supplementary Material: Supplementary Methods and Results). This patient had been previously diagnosed with mixed Hodgkin and follicular lymphoma. In

2020, the patient developed severe SARS-CoV-2-associated pneumonia as diagnosed virologically by qPCR. Despite clinical improvement, viral clearance did not occur as SARS-CoV-2 RNA remained detectable by qPCR on most nasopharyngeal samples collected until patient's death. qPCR was negative at Month 5 of diagnosis but positive when re-tested at Month 7, and then only transiently negative for ≤3 days.

Evidence of hybrids of variants

After 14 months of infection, we identified a virus whose genome was a hybrid of two known variants, B.1.160 [according to Pangolin lineage (https://cov-lineages.org/resources/pangolin.html) [31]] [a.k.a. Nextstrain clade (https://nextstrain.org/) [32] 20A.EU2, or Marseille-4 [27]] and Alpha [according to the WHO denomination (https://www.who.int/fr/activities/tracking-SARS-CoV-2-variants) (a.k.a. 20I or B.1.1.7)] (Figure 1; Figure 2).

This hybrid genome was obtained from the respiratory samples by next-generation sequencing, as previously described [27]. In addition, the hybrid virus was isolated in culture, as previously described [33]. The hybrid genome sequence consisted of a B.1.160 variant matrix, of which two regions, the first one being located at the 5' tip of the ge-nome and containing synonymous mutation C913U and the second one spanning from positions 17,109-18,877 to positions 25,710-27,972, were replaced by those of an Alpha variant (Figure 1; Figure 2; Supplementary Material: Figure S1). All eight signature mu-tations of the Alpha variant were detected in the spike gene in the absence of the S477N mutation that is a signature of the B.1.160 variant. Nucleotide diversity at the 35 positions harboring signature mutations of the Alpha or B.1.160 variants was low [mean (±standard deviation) value of 3.1±6.8%] (Figure 2; Supplementary Material: Figure S1), indicating that the hybrid content of the genome was not explained by a co-infection by the two variants or by contamination. These findings indicated that this mosaic genome was the result of recombinations between parental genomes of the B.1.160 and Alpha variants.

Genome of the initial virus

By analyzing the sequential samples available from this patient, we were able to determine that he was first infected with the B.1.160 variant, which was epidemic at the time of diagnosis of his infection during summer 2020. This variant predominated in our region from August 2020 until January 2021 and was replaced by the Alpha variant that emerged in December 2020 [27]. SARS-CoV-2 could not be isolated retrospectively from this sample, but its genome was typical of a B.1.160 variant and displayed no significant nucleotide diversity (mean, 0.2±0.5%). It was classified by phylogeny as a B.1.160 variant (Figure 3). Unfortunately, although SARS-CoV-2 qPCR was still positive in another laboratory at Month 4 post-diagnosis, the sample was unavailable, and we were not able to verify that only this virus had persisted and that there was no co-infection with an Alpha variant at this time. Thus, we did not obtain the genome and an isolate of the Alpha variant. The closest sample in time to the initial one dated from Month 8, and it already demonstrated a mosaicism between genomes of B.1.160 and Alpha variants (Figure 1, Figure 2).

Steps in creation of the recombinant

We used three procedures to characterize the different recombination steps by analyzing seven sequential respiratory samples collected from the patient (Tables 1, 2). First, sequencing from the respiratory samples of the viral genomes; second, sequencing from the respiratory samples of PCR products overlapping the putative recombination sites; and third, viral culture with sequencing of the genomes of the isolates. These approaches allowed us to evidence that several viruses and recombinant forms had coexisted in the sequential samples, as signature mutations of the two variants were co-detected at multiple positions, with a nucleotide diversity that reached high levels and evolved over time (Figure 2; Supplementary Material: Supplementary Results and Figure S1). We observed an evolution towards the genome sequence of the recombinant virus that predominated at the end of the patient's follow-up, following recombination events at three sites between parental genomes of B.1.160

and Alpha variants, with a low level of nucleotide diversity observed at that time at the positions harboring signature mutations of these variants.

DISCUSSION

We highlight here in an immunocompromised lymphoma patient who received several treatments the presence after 14 months of infection of a hybrid virus of two known variants, B.1.160 and Alpha, which successively predominated in our region during the period during which this patient was followed-up [35, 27]. The first evidence of a hybrid genome was obtained 8 months after the diagnosis of infection by the B.1.160 variant, and the absence of available samples covering this period did not allow us to date the superinfection by the Alpha variant. The signature mutations of the Alpha variant observed in the hybrid genomes between 8 and 14 months cannot have occurred randomly considering their number and distribution along the genome and their majority presence, and their location indicates recombinations in three regions. In addition, genomic analyses carried out for sequential respiratory samples and viral cultures demonstrate the successive presence of several viruses with hybrid genomes, one of them having established itself in this patient and remaining the one that continued circulating until his death.

We believe that this observation, which sheds light on the recombination mecha-nism of RNA viruses, is significant, and to our knowledge this is the first one describing, through the analysis of sequential samples over more than a year, the creation of a re-combinant SARS-CoV-2 and the isolation of the recombinant virus in culture. Sixteen interlineage recombinants between the Alpha variant and non-Alpha viruses were reported in 2021 in the UK, of 279,000 genomes analyzed [8]. In addition, 1,175 (0.2%) pu-tative recombinant genomes were identified among 537,360 genomes, and it was reported that up to 5% of SARS-CoV-2 that circulated in the USA and UK might be recombinants [18]. Moreover, the number of cases of detection of recombinant genomes is growing [10,13-14,15-25]. Recently,

coronaviruses have been reported to be able to integrate se-quences putatively from insects [36]. Such natural mosaicisms in these viruses make it possible to understand the emergence of RNA viruses and should lead to a strengthening of genomic surveillance in patients presenting with coinfections by several RNA viruses, as is observed in patients infected with several respiratory viruses including SARS-CoV-2, endemic human coronaviruses, influenza viruses, or rhinoviruses [37]. Such infectious episodes could perhaps lead to the creation of new emerging viruses, as has been for instance reported for enteroviruses of humans and great apes [38].

MATERIALS AND METHODS

SARS-CoV-2 genome sequencing

SARS-CoV-2 genome sequencing was performed as previously described. Briefly, viral RNA was extracted from 200 µL of nasopharyngeal swab fluid using the EZ1 Virus Mini kit v2.0 on an EZ1 Advanced XL instrument (Qiagen, Courtaboeuf, France) or using the MagMax Viral/Pathogen Nucleic Acid Isolation kit on the KingFisher Flex system (Thermo Fisher Scientific, Waltham, MA, United States), following the manufacturer's instructions. SARS-CoV-2 genome sequences were obtained by next-generation sequencing with various procedures with the Illumina COVIDSeq protocol on a NovaSeq 6000 instrument (Illumina Inc.), or by multiplex PCR with ARTIC nCoV-2019 V3 Panel primers (IDT, Coralville, IA, USA) combined with the Oxford Nanopore technology (ONT) on a GridION instrument (Oxford Nanopore Technologies Ltd., Oxford, United Kingdom), as previously described [27,14]. After its extraction, viral RNA was reverse-transcribed according to the COVIDSeq protocol (Illumina Inc.) or using the LunaScript RT SuperMix kit (New England Biolabs) when performing next-generation sequencing with the Nanopore technology, following the manufacturer's recommendations.

Genome analysis

After using the Nanopore technology combined with the ARTIC protocol, fastq files were processed using the ARTIC field bioinformatics pipeline (ARTIC-nCoV-bioinformaticsSOP-v1.1.0; https://github.com/artic-network/fieldbioinformatics), as previously described [27,14]. NGS reads were basecalled using Guppy (4.0.14) and aligned to the genome of the Wuhan-Hu-1isolate, GenBank accession No. MN908947.3, using minimap2 (v2.17-r941) (https://github.com/lh3/ minimap2) [39]. The ARTIC tool align_trim was used to softmask primers from read alignment and cap sequencing depth at a maximum of 400-fold coverage. Consensus-level variant candidates were identified using a threshold of 70% and the Medaka (v.0.11.5) workflow developed by ARTIC (https://github.com/artic-network/artic-ncov2019). From the unique sequence obtained with the ARTIC-Nanopore technology, a sorted bam file was loaded on the CLC Genomics workbench v7 software and a tsv file was then exported. NovaSeq reads were basecalled using the Dragen Bcl Convert pipeline (v3.9.3; https://emea.support.illumina.com/sequencing/sequencing_software/bcl-convert.html (Illumina Inc.)). Mapping was carried out on the Wuhan-Hu-1 isolate genome with the bwa-mem2 tool (v2.2.1; https://github.com/bwa-mem2/bwa-mem2) and was cleaned with Samtools (v1.13; https://www.htslib.org/) [40]. Variant calling was performed with freebayes (v1.3.5; https://github.com/freebayes/freebayes) [41] and consensus genomes were built with Bcftools (v1.13; https://samtools.github.io/bcftools/bcftools.html). Freebayes results were filtered with a threshold of 70% for the majority nucleotide. A tsv file was generated using an in-house Python script. The clade was designated at the consensus level with the Nextclade online tool (https://clades.nextstrain.org/) [42,32] and an in-house Python script allowed detection of variants and hybrids of variants. At the sub-consensus level, variant frequencies compared to the Wuhan-Hu-1 isolate genome were calculated from tsv files. Nucleotide diversity at genomic positions was calculated using the Microsoft Excel software (https://www.microsoft.com/en-us/microsoft-365/excel) with an in-house built file. It corresponded to the proportion of sequence reads that do not harbor the consensus

(majority) nucleotide. Genome sequences obtained in the present study were submitted to the GISAID sequence database (https://www.gisaid.org/) [34] (see Supplementary Material: Supplementary Table S1).

Generation of additional sequence reads

Sequencing of reverse-transcription-PCR-targeted regions: Extraction of the RNA samples was carried out using the EZ1 Virus kit with the EZ1 Advanced XL instrument (Qiagen) following the manufacturer's recommendations. PCR amplification of the 3 regions was amplified in a 25 µL total volume using the SuperScript III One-Step RT-PCR Kit (Invitrogen, Carlsbad, CA, USA), using primer concentrations of 200 nM per reaction. PCR were performed with following conditions: 50°C for 25 min, 95°C for 2 min, then 40 cycles including 15 s at 95°C, 45 s at 60°C, and 2 min at 68°C. Sequences of PCR primers are provided in the Supplementary Material. Amplicons were sequenced with Nanopore technology on a GridION instrument (Oxford Nanopore Technologies Ltd.), following manufacturer's instructions. Fastq files were processed as described above. Continuous reads overlapping signature mutations of distinct variants were filtered using SAMtools (v1.13; https://github.com/samtools/) [40] combined with an in-house awk script. Reads were then filtered according to variant-specific nucleotide patterns using SAMtools combined with an in-house awk script. Groups of reads with same patterns of mutations were then visualized using the IGV software (https://software.broadinstitute.org/software/igv/) [43].

Metagenomic sequencing: Nucleic acid extraction was performed with the EZ1 Virus kit with the EZ1 Advanced XL instrument (Qiagen) following the manufacturer's recommendations, using 200 µL of sample and eluting in 60 µL of elution buffer. Reverse transcription was performed with all 60 µL of this solution using the TaqMan Reverse Transcription Reagent kit (Applied-Biosystems, Foster City, CA, USA), according to the manufacturer's protocol under the following conditions: 10 min at 25°C, 30 min at 48°C, and 5 min at 95°C. Then, 300 µL of obtained cDNA was transferred in a 1.5 mL Eppendorf

LoBind tube (Eppendorf, Le Pecq, France). Second DNA strand was synthesized by adding a mix of 24 µL of Klenow Fragment DNA polymerase (New England Biolabs, Beverly, MA, USA), 66 µL of nuclease-free water, 45 µL of NEB Buffer 2 (New England Biolabs), and 15 µL of dNTPs working solution produced with 10 µL of each dNTP at a 100 mM concentration, and 60 µL of nuclease-free water (New England Biolabs). This mix was kept at 37°C for one hour. A purification step consisted in adding 450 µL of magnetic CleanNGS beads for a 1:1 volume ratio (CleanNA, Waddinxveen, the Netherlands) then incubating for 5 min in a magnetic support, and washing with 1,000 µL of ethanol at 70%, before elution of beads in 50 µL of Tris EDTA 1X with centrifugation for 10 min at 300 rpm at room temperature. Subsequently, DNA library was prepared with the DNA ligation sequencing kit SQK-LSK109 (Oxford Nanopore Technologies Ltd.), and next-generation sequencing was performed with the Nanopore technology on a PromethION instrument (Oxford Nanopore Technologies Ltd.). Each sample was sequenced on a different PromethION Flow cell R10.4 (Oxford Nanopore Technologies Ltd.).

Phylogenetic analysis on whole and partial genomes

Phylogenetic analyses were performed separately for the twelve genome sequences and the twelve spike gene sequences obtained from the nasopharyngeal samples or the culture supernatants. Sequences were aligned using MAFFT v.7 [44] with their 20 most similar hits identified with the BLAST tool [45] among SARS-CoV-2 genomes from our database that contains sequences obtained from clinical samples collected between February 2020 and February 2022 [27,14]. Phylogeny reconstruction was performed using the IQ-TREE software with the GTR Model and 1,000 ultrafast bootstrap repetitions (http://www.iqtree.org) [46], and trees were visualized with iTOL (Interactive Tree Of Life) (https://itol.embl.de/) [47] and MEGA X (v10.2.6; https://www.megasoftware.net/) [47] softwares.

Virus culture isolation

Culture isolation was performed on Vero E6 cells, as previously described [33].

Acknowledgments

We are thankful to Ludivine Brechard, Claudia Andrieu, Raphael Tola, Jeremy Delerce for their technical help; to Sophie Amrane and Justine Raclot for their help with the clinical management; and to the medical biology laboratory Alphabio, hôpital Européen, Marseille, France, for providing some results of SARS-CoV-2 qPCR testing.

Author contributions

P.C., B.L.S., and D.R. conceived the project. E.B., P.C., J.-C.L., A.L., M.B., and P.L. provided materials or performed analyses. E.B., P.C., J.-C.L., A.L., M.B., P.-E.F., B.L.S., and D.R. analyzed the data. E.B., P.C., P.-E.F., B.L.S, and D.R. drafted the paper. All authors participated in the discussion and interpretation of the results. All authors edited and proofread the final manuscript. All authors have read and agreed to the published version of the manuscript.

Funding

This work was supported by the French Government under the “Investments for the Future” program managed by the National Agency for Research (ANR) (Méditerranée-Infection 10-IAHU-03), by the Région Provence Alpes Côte d’Azur and European funding FEDER PRIMMI (Fonds Européen de Développement Régional-Plateformes de Recherche et d'Innovation Mutualisées Méditerranée Infection) (FEDER PA 0000320 PRIMMI), and by the French Ministry of Higher Education, Research and Innovation (ministère de l'Enseignement supérieur, de la Recherche et de l'Innovation) and the French Ministry of Solidarity and Health (Ministère des Solidarités et de la Santé).

Data availability

The dataset generated and analyzed during the current study is available in the GISAID sequence database (https://www.gisaid.org/) [34].

Conflicts of interest

The authors have no conflicts of interest to declare relative to the present study. Didier Raoult was a consultant for the Hitachi High-Technologies Corporation, Tokyo, Japan from 2018 to 2020. He is a scientific board member of the Eurofins company and a founder of a microbial culture company (Culture Top). Funding sources had no role in the design and con-duct of the study, the collection, management, analysis, and interpretation of the data, and the preparation, review, or approval of the manuscript.

Ethics

This study has been approved by the ethics committee of University Hospital Institute (IHU) Méditerranée Infection (No. 2022-008). Access to the patients' biological and registry data issued from the hospital information system was approved by the data protection committee of Assistance Publique-Hôpitaux de Marseille (APHM) and was recorded in the European General Data Protection Regulation registry under number RGPD/APHM 2019-73.

REFERENCES

1. Xiao, Y.; Rouzine, IM.; Bianco S.; et al. RNA Recombination Enhances Adaptability and Is Required for Virus Spread and Virulence. Cell Host Microbe. 2017, 22, 420. doi: 10.1016/j.chom.2017.08.006.
2. Bentley, K.; Evans, D.J. Mechanisms and consequences of positive-strand RNA virus recombination. J Gen Virol. 2018, 99, 1345-1356. doi: 10.1099/jgv.0.001142.
3. Lai, MMC. Recombination in large RNA viruses: Coronaviruses. Semin Virol. 1996, 7, 381-388.
4. Zhang, Y.; Li, J.; Xiao, Y.; et al. Genotype shift in human coronavirus OC43 and emergence of a novel genotype by natural recombination. J Infect. 2015, 70, 641-50.
5. So, RTY.; Chu, DKW.; Miguel, E.; et al. Diversity of Dromedary Camel Coronavirus HKU23 in African Camels Revealed Multiple Recombination Events among Closely Related Betacoronaviruses of the Subgenus Embecovirus. J Virol. 2019, 93, e01236-19. doi: 10.1128/JVI.01236-19.
6. Gribble, J.; Stevens, L.J.; Agostini, M.L.; et al. The coronavirus proofreading exoribonuclease mediates extensive viral recombination. PLoS Pathog. 2021, 17, e1009226. doi: 10.1371/journal.ppat.1009226.
7. Zhu, Z.; Meng, K.; Meng, G. Genomic recombination events may reveal the evolution of coronavirus and the origin of SARS-CoV-2. Sci Rep. 2020, 10, 21617. doi: 10.1038/s41598-020-78703-6.
8. Jackson, B.; Boni, MF.; Bull, MJ.; et al. Generation and transmission of interlineage recombinants in the SARS-CoV-2 pandemic. Cell. 2021, 184, 5179-5188.e8.
9. Francisco, R.D.S. Jr.; Benites, L.F.; Lamarca, A.P.; et al. Pervasive transmission of E484K and emergence of VUI-NP13L with evidence of SARS-CoV-2 co-infection

events by two different lineages in Rio Grande do Sul, Brazil. Virus Res. 2021, 296, 198345. doi: 10.1016/j.virusres.2021.198345.

10. Taghizadeh, P.; Salehi, S.; Heshmati, A.; et al. Study on SARS-CoV-2 strains in Iran reveals potential contribution of co-infection with and recombination between different strains to the emergence of new strains. Virology. 2021, 562, 63-73. doi: 10.1016/j.virol.2021.06.004.

11. Rockett, J.D.; Gall, M.; Sim, E.M.; et al. Co-infection with SARS-CoV-2 Omicron and Delta Variants revealed by genomic surveillance. medRxiv 2022, 2022.02.13.22270755; doi: https://doi.org/10.1101/2022.02.13.22270755.

12. Musso, N.; Maugeri, J.G.; Bongiorno, D.; et al. SARS-CoV-2's high rate of genetic mutation under immune selective pressure: from oropharyngeal B.1.1.7 to intrapulmonary B.1.533 in a post-vaccine patient. Int J Infect Dis. 2022, S1201-9712(22)00123-0. doi: 10.1016/j.ijid.2022.02.044.

13. He, Y.; Ma, W.; Dang, S.; et al. Possible recombination between two variants of concern in a COVID-19 patient. Emerg Microbes Infect. 2022, 11, 552-555. doi: 10.1080/22221751.2022.2032375.

14. Colson, P.; Fournier, P.E.; Delerce, J.; et al. Culture and identification of a “Deltamicron” SARS-CoV-2 in a three cases cluster in southern France medRxiv 2022, 2022.03.03.22271812; doi: https://doi.org/10.1101/2022.03.03.22271812

15. Yi, H. 2019 Novel Coronavirus Is Undergoing Active Recombination. Clin Infect Dis. 2020, 71, 884-887. doi: 10.1093/cid/ciaa219.

16. Yeh, T.Y.; Contreras, G.P. Emerging viral mutants in Australia suggest RNA recombination event in the SARS-CoV-2 genome. Med J Aust. 2020, 213, 44-44.e1. doi: 10.5694/mja2.50657. Epub 2020 Jun 7. PMID: 32506536; PMCID: PMC7300921.

17. Gallaher, W.R. A palindromic RNA sequence as a common breakpoint contributor to copy-choice recombination in SARS-COV-2. Arch Virol. 2020, 165, 2341-2348. doi: 10.1007/s00705-020-04750-z.
18. VanInsberghe, D.; Neish, A.S.; Lowen, A.C.; Koelle, K. Recombinant SARS-CoV-2 genomes are currently circulating at low levels. bioRxiv. 2021 Mar 15:2020.08.05.238386. doi: 10.1101/2020.08.05.238386.
19. Haddad, D.; John, S.E.; Mohammad, A.; et al. SARS-CoV-2: Possible recombination and emergence of potentially more virulent strains. PLoS One. 2021, 16, e0251368.
20. Varabyou, A.; Pockrandt, C.; Salzberg, S.L.; Pertea, M. Rapid detection of inter-clade recombination in SARS-CoV-2 with Bolotie. Genetics. 2021, 218, iyab074. doi: 10.1093/genetics/iyab074.
21. Leary, S.; Gaudieri, S.; Parker, M.D.; et al. Generation of a novel SARS-CoV-2 sub-genomic RNA due to the R203K/G204R variant in nucleocapsid: homologous recombination has potential to change SARS-CoV-2 at both protein and RNA level. bioRxiv. 2021 Aug 6:2020.04.10.029454. doi: 10.1101/2020.04.10.029454. Update in: Pathog Immun. 2021 Aug 20;6(2):27-49.
22. Lohrasbi-Nejad, A. Detection of homologous recombination events in SARS-CoV-2. Biotechnol Lett. 2022, 17, 1–16. doi: 10.1007/s10529-021-03218-7.
23. Kreier, F. Deltacron: the story of the variant that wasn't. Nature. 2022, 602, 19.
24. Ignatieva, A.; Hein, J.; Jenkins, P.A. Ongoing Recombination in SARS-CoV-2 Revealed through Genealogical Reconstruction. Mol Biol Evol. 2022, 39, msac028. doi: 10.1093/molbev/msac028.
25. Sekizuka, T.; Itokawa, K.; Saito, M.; et al. Genome Recombination between Delta and Alpha Variants of Severe Acute Respiratory Syndrome Coronavirus 2 (SARS-CoV-2). Jpn J Infect Dis. 2022 Feb 28. doi: 10.7883/yoken.JJID.2021.844.

26. Million, M.; Lagier, J.C.; Tissot-Dupont, H.; et al. Early combination therapy with hydroxychloroquine and azithromycin reduces mortality in 10,429 COVID-19 outpatients. Rev Cardiovasc Med. 2021, 22, 1063-1072. doi: 10.31083/j.rcm2203116.

27. Colson, P.; Fournier, PE.; Chaudet, H.; et al. Analysis of SARS-CoV-2 Variants From 24,181 Patients Exemplifies the Role of Globalization and Zoonosis in Pandemics. Front Microbiol. 2022, 12, 786233. doi: 10.3389/fmicb.2021.786233.

28. Brouqui, P.; Colson, P.; Melenotte, C.; et al. COVID-19 re-infection. Eur J Clin Invest. 2021, 51, e13537. doi: 10.1111/eci.13537.

29. Drancourt, M.; Cortaredona, S.; Melenotte, C.; et al. SARS-CoV-2 Persistent Viral Shedding in the Context of Hydroxychloroquine-Azithromycin Treatment. Viruses. 2021, 13, 890. doi: 10.3390/v13050890.

30. Colson, P.; Devaux, C.A.; Lagier, J.C.; Gautret, P.; Raoult, D. A Possible Role of Remdesivir and Plasma Therapy in the Selective Sweep and Emergence of New SARS-CoV-2 Variants. J Clin Med. 2021, 10, 3276. doi: 10.3390/jcm10153276.

31. Rambaut, A.; Holmes, E.C.; O'Toole, A.; et al. A dynamic nomenclature proposal for SARS-CoV-2 lineages to assist genomic epidemiology. Nat Microbiol. 2020, 5, 1403-1407. doi: 10.1038/s41564-020-0770-5.

32. Aksamentov, I.; Roemer, C.; Hodcroft, E.B.; Neher, R.A. Nextclade: clade assignment, mutation calling and quality control for viral genomes. Zenodo 2021, https://doi.org/10.5281/zenodo.5607694.

33. La Scola, B.; Le Bideau, M.; Andreani, J.; et al. Viral RNA load as determined by cell culture as a management tool for discharge of SARS-CoV-2 patients from infectious disease wards. Eur J Clin Microbiol Infect Dis. 2020, 39, 1059-1061.

34. Alm, E.; Broberg, EK.; Connor, T.; et al. Geographical and temporal distribution of SARS-CoV-2 clades in the WHO European Region, January to June 2020. Euro Surveill. 2020, 25, 2001410.

35. Fournier, P.E.; Colson, P.; Levasseur, A.; et al. Emergence and outcomes of the SARS-CoV-2 'Marseille-4' variant. Int J Infect Dis. 2021, 106, 228-236.
36. Tengs, T.; Delwiche, C.F.; Monceyron Jonassen, C. A genetic element in the SARS-CoV-2 genome is shared with multiple insect species. J Gen Virol. 2021, 102, 001551.
37. Le Glass, E.; Hoang, V.T.; Boschi, C.; et al. Incidence and Outcome of Coinfections with SARS-CoV-2 and Rhinovirus. Viruses. 2021, 13, 2528.
38. Amona, I.; Medkour, H.; Akiana, J.; et al. Enteroviruses from Humans and Great Apes in the Republic of Congo: Recombination within Enterovirus C Serotypes. Microorganisms. 2020, 8, 1779.
39. Li, H. Minimap2: pairwise alignment for nucleotide sequences. Bioinformatics. 2018, 34, 3094-3100. doi:10.1093/bioinformatics/bty191
40. Hadfield, J.; Megill, C.; Bell, S.M.; Huddleston, J.; Potter, B.; Callender, C. Nextstrain: real-time tracking of pathogen evolution. Bioinformatics. 2018, 34, 4121–4123.
41. Danecek, P.; Bonfield, J.K.; Liddle, J.; et al. Twelve years of SAMtools and BCFtools, GigaScience 2021, 10, giab008, https://doi.org/10.1093/gigascience/giab008.
42. Garrison, E.; Marth, G. Haplotype-based variant detection from short-read sequencing. arXiv.org 2012, https://arxiv.org/abs/1207.3907.
43. Robinson, J.T.; Thorvaldsdottir, H.; Wenger, A.M.; Zehir, A.; Mesirov, J.P. Variant Review with the Integrative Genomics Viewer (IGV). Cancer Research 2017, 77, 31-34.
44. Katoh, K.; Standley, D.M. MAFFT multiple sequence alignment software version 7: improvements in performance and usability. Mol Biol Evol. 2013, 30, 772-780. doi:10.1093/molbev/mst010
45. Altschul, S.F.; Gish, W.; Miller, W.; Myers, EW.; Lipman, D.J. Basic local alignment search tool. J Mol Biol. 1990, 215, 403-10. doi: 10.1016/S0022-2836(05)80360-2.
46. Minh, B.Q.; Schmidt, H.A.; Chernomor, O.; et al. IQ-TREE 2: New Models and Efficient Methods for Phylogenetic Inference in the Genomic Era [published correction

appears in Mol Biol Evol. 2020 Aug 1;37(8):2461]. Mol Biol Evol. 2020, 37, 1530-1534. doi:10.1093/molbev/msaa015

47. Letunic, I.; Bork, P. Interactive tree of life (iTOL) v3: an online tool for the display and annotation of phylogenetic and other trees. Nucleic Acids Res. 2016, 44, W242-W245. doi:10.1093/nar/gkw290

48. Kumar, S.; Stecher, G.; Li, M.; Knyaz, C. Tamura K. MEGA X: Molecular Evolutionary Genetics Analysis across Computing Platforms. Mol Biol Evol. 2018, 35, 1547-1549. doi: 10.1093/molbev/msy096.

FIGURE LEGEND

Figure 1. Schematic representation of the structure of the SARS-CoV-2 genomes obtained from the nasopharyngeal samples and from the culture supernatants and of the recombination events over time, in reference to parental genomes of the B.1.160 and Alpha variants.

a. Genome map and annotation. b. Genome structure and mutations. Blue color of rectangles indicates sequences from a B.1.160 variant; yellow color indicates sequences from an Alpha variant; green color indicates co-detection of sequences from a B.1.160 variant and from an Alpha variant; grey color indicates sequences from indeterminate origin. Signature mutations from the B.1.160 and Alpha variants are indicated by a blue background and a yellow background, respectively. Signature mutations that are absent are indicated by a red font. Δ21765: -6 nucleotides; Δ21991: -3 nucleotides. Nsp, nonstructural protein; ORF, open reading frame.

Figure 2. Majority nucleotides (a) and nucleotide diversity (b) for sequences obtained from the respiratory samples and the culture supernatant at nucleotide positions of the SARS-CoV-2 genome that harbor signature mutations of the B.1.160 or Alpha variants.

Nucleotide positions are in reference to the genome of the Wuhan-Hu-1 isolate GenBank accession no. NC_045512.2.

a: B.1.160 nucleotides are indicated by a blue background; Alpha nucleotides are indicated by a yellow background. Del, nucleotide deletion

b: Nucleotide diversity is the proportion of sequence reads that do not harbor the consensus (majority) nucleotide.

Figure 3. Phylogenetic analyses based on SARS-CoV-2 genomes (a) and spike gene

sequences (b).

Sequences obtained from the case-patient are indicated by a grey background, and those obtained from cultures are underlined. Other sequences from our SARS-CoV-2 sequence database are indicated by a blue font when classified as of the B.1.160 variant, and by a yellow font when classified as of the Alpha variant. Sequences are labeled with their GISAID (https://www.gisaid.org/) [34] identifiers. Trees are rooted with the genome of the Wuhan-Hu-1 isolate GenBank accession no. NC_045512.2.

TABLE

Table 1. Genome sequences obtained from the sequential nasopharyngeal samples of the case-patient

GISAID identifier	Sampling time post-diagnosis (months)	Next-generation sequencing technology, instrument
EPI_ISL_6332079	M0	Illumina, NovaSeq
EPI_ISL_10816743	Month 8	Illumina, NovaSeq
EPI_ISL_11030507	Month 9	Illumina, NovaSeq
EPI_ISL_10816731	Month 10	Illumina, NovaSeq
EPI_ISL_10816742	Month 11	Nanopore, GridION
EPI_ISL_10816744	Month 13	Illumina, NovaSeq
EPI_ISL_10816733	Month 14	Illumina, NovaSeq

Table 2. Genome sequences obtained from the culture supernatants

GISAID identifier	Sampling date of the nasopharyngeal sample	Time to cytopathic effect (days)	Next-generation sequencing technology, instrument
EPI_ISL_10816730	Month 8	8	Illumina, NovaSeq
EPI_ISL_10816732	Month 9	4	Illumina, NovaSeq
EPI_ISL_10816734	Month 11	4	Illumina, NovaSeq
EPI_ISL_10816735	Month 14	5	Illumina, NovaSeq
EPI_ISL_10816738	Month 14	7	Illumina, NovaSeq

Fig. 1

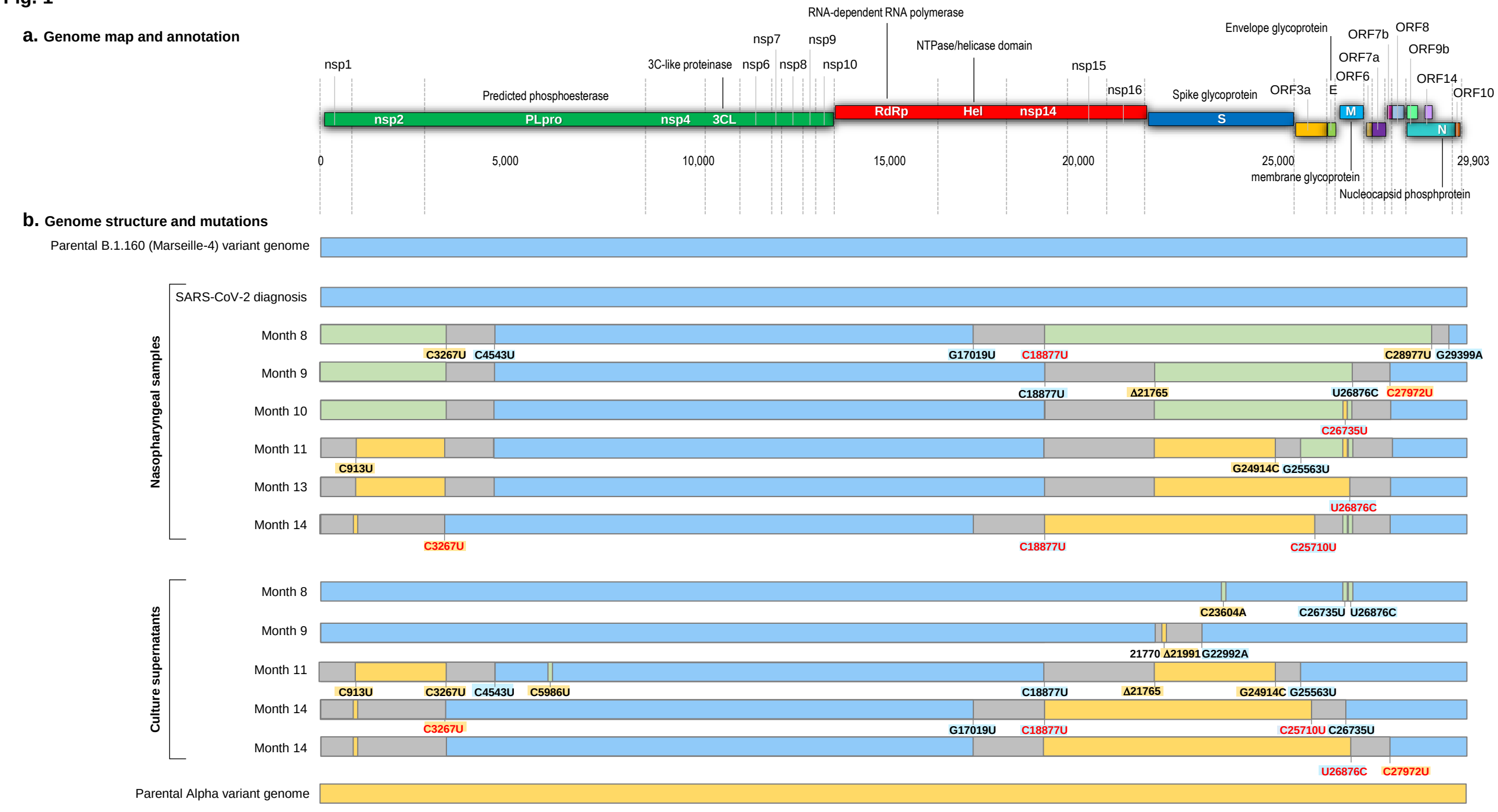
a. Genome map and annotation
RNA-dependent RNA polymerase
nsp7
nsp9
NTPase/helicase domain
Envelope glycoprotein
ORF7b
ORF8
nsp1
3C-like proteinase
nsp6
nsp8
nsp10
nsp15
ORF7a
ORF9b
ORF6
ORF14
nsp16
Spike glycoprotein
ORF3a
E
ORF10
Predicted phosphoesterase
nsp2
PLpro
nsp4
3CL
RdRp
Hel
nsp14
S
M
N
0
5,000
10,000
15,000
20,000
25,000
29,903
membrane glycoprotein
Nucleocapsid phosphprotein
b. Genome structure and mutations
Parental B.1.160 (Marseille-4) variant genome
Nasopharyngeal samples
SARS-CoV-2 diagnosis
Month 8
C3267U C4543U G17019U C18877U C28977U G29399A
Month 9
C18877U Δ21765 U26876C C27972U
Month 10
C26735U
Month 11
C913U G24914C G25563U
Month 13
U26876C
Month 14
C3267U C18877U C25710U
Culture supernatants
Month 8
C23604A C26735U U26876C
Month 9
21770 Δ21991 G22992A
Month 11
C913U C3267U C4543U C5986U C18877U Δ21765 G24914C G25563U
Month 14
C3267U G17019U C18877U C25710U C26735U
Month 14
U26876C C27972U
Parental Alpha variant genome

Fig. 2

a.

Nucleotide positions	Wuhan-Hu-1 isolate genome	Signature mutations in B.1.160/Marseille-4 genomes	Signature mutations in Alpha genomes	Majority nucleotides: Nasopharyngeal samples: SARS-CoV-2 diagnosis	Month 8	Month 9	Month 10	Month 11	Month 13	Month 14	Culture supernatants: Month 8	Month 9	Month 11	Month 14	Month 14
913	C	-	U	-	-	-	U	U	U	U	-	-	U	U	U
3267	C	-	U	-	-	-	U	U	U	-	-	-	U	-	-
4543	C	U	-	U	U	U	U	U	U	U	U	U	U	U	U
5629	G	U	-	U	U	U	U	U	U	U	U	U	U	U	U
5986	C	-	U	-	-	-	-	-	-	-	-	-	U	-	-
9526	G	U	-	U	U	U	U	U	U	U	U	U	U	U	U
11497	C	U	-	U	U	U	U	U	U	U	U	U	U	U	U
13993	G	U	-	U	U	U	U	U	U	U	U	U	U	U	U
15766	G	U	-	U	U	U	U	U	U	U	U	U	U	U	U
16889	A	G	-	G	G	G	G	G	G	G	G	G	G	G	G
17019	G	U	-	U	U	U	U	U	U	U	U	U	U	U	U
18877	C	U	-	U	-	U	U	U	U	-	U	U	U	-	-
21765	U	-	Del	-	-	-	-	Del	Del	Del	-	-	Del	Del	Del
21766	A	-	Del	-	-	-	-	Del	Del	Del	-	-	Del	Del	Del
21767	C	-	Del	-	-	-	-	Del	Del	Del	-	-	Del	Del	Del
21768	A	-	Del	-	-	-	-	Del	Del	Del	-	-	Del	Del	Del
21769	U	-	Del	-	-	-	-	Del	Del	Del	-	-	Del	Del	Del
21770	G	-	Del	-	-	-	-	Del	Del	Del	-	-	Del	Del	Del
21991	U	-	Del	-	-	Del	Del	Del	Del	Del	-	Del	Del	Del	Del
21992	U	-	Del	-	-	Del	Del	Del	Del	Del	-	Del	Del	Del	Del
21993	A	-	Del	-	-	Del	Del	Del	Del	Del	-	Del	Del	Del	Del
22992	G	A	-	A	A	/	-	-	-	-	A	A	-	-	-
23063	A	-	U	-	-	-	U	U	U	U	-	-	U	U	U
23271	C	-	A	-	-	-	A	A	A	A	-	-	A	A	A
23604	C	-	A	-	-	-	A	A	A	A	A	-	A	A	A
23709	C	-	U	-	-	-	U	U	U	U	-	-	U	U	U
24506	U	-	G	-	-	-	G	G	G	G	-	-	G	G	G
24914	G	-	C	-	-	-	C	C	C	C	-	-	C	C	C
25563	G	U	-	U	U	U	-	U	-	-	U	U	U	-	-
25710	C	U	-	U	-	U	-	U	-	-	U	U	U	-	-
26735	C	U	-	U	-	-	-	-	-	-	U	U	U	U	-
26876	U	C	-	C	-	-	-	C	-	-	C	C	C	C	-
28975	G	C	-	C	-	C	C	C	C	C	C	C	C	C	C
28977	C	-	U	-	U	-	-	-	-	-	-	-	-	-	-
29399	G	A	-	A	A	A	A	A	A	A	A	A	A	A	A

b.

Nucleotide diversity (%): Nasopharyngeal samples: SARS-CoV-2 diagnosis	Month 8	Month 9	Month 10	Month 11	Month 13	Month 14	Culture supernatants: Month 8	Month 9	Month 11	Month 14	Month 14
0,0	33,9	26,8	35,9	10,0	0,1	0,1	9,0	0,1	0,1	0,1	0,3
0,0	28,8	23,7	39,3	6,8	0,0	0,0	2,4	0,1	0,2	0,4	0,1
0,1	0,0	0,0	0,0	7,8	0,0	0,1	0,3	0,2	0,2	0,8	0,1
2,8	0,5	1,6	0,2	11,4	0,6	0,0	0,8	1,9	0,9	5,3	1,5
0,0	0,0	0,0	0,0	10,3	0,0	0,0	0,0	0,0	18,4	0,0	0,1
0,1	0,0	0,0	0,0	4,6	0,0	0,8	1,2	0,2	0,2	0,0	0,3
0,4	0,0	0,0	0,3	2,5	0,4	0,0	0,1	0,3	0,2	0,1	0,2
0,1	0,1	0,0	0,1	5,4	0,1	0,0	0,0	0,1	0,0	0,3	0,1
0,1	0,3	0,0	0,1	9,2	0,0	0,0	0,0	0,1	0,0	0,1	0,1
0,1	0,0	0,0	0,0	7,7	0,0	0,2	0,0	0,1	0,0	0,3	0,1
0,0	0,0	0,0	0,0	15,6	0,0	0,0	0,3	0,2	0,4	0,1	0,1
0,0	47,0	0,0	0,0	6,8	0,0	0,1	2,7	0,2	0,0	0,2	0,1
0,1	14,7	11,0	38,3	39,2	22,6	22,9	2,1	0,0	21,8	23,7	21,2
0,0	16,2	11,8	44,0	10,9	1,6	1,1	2,2	0,0	1,2	1,6	1,0
0,1	15,4	11,1	42,8	19,6	0,0	0,0	2,1	0,0	0,0	0,1	0,0
0,0	15,4	11,2	43,1	10,4	0,0	0,0	2,1	0,0	0,0	0,1	0,1
0,0	15,6	11,5	43,7	13,7	0,2	0,2	2,1	0,1	0,2	0,5	0,5
0,1	18,2	15,2	47,6	9,6	5,6	5,6	3,6	0,0	7,2	6,4	6,5
0,0	20,3	17,3	18,6	22,1	1,3	4,3	0,1	2,1	2,5	0,7	1,4
0,1	20,4	16,9	18,1	20,3	1,3	5,6	0,1	2,1	2,5	2,0	2,1
0,1	20,6	16,7	17,7	17,8	3,7	18,9	0,1	11,5	7,4	10,7	12,6
0,3	33,3	/	20,6	4,8	0,0	0,0	5,5	0,1	0,0	0,2	0,3
0,0	50,0	33,3	27,1	12,4	0,0	0,0	6,7	0,1	0,0	0,4	0,4
0,2	15,7	20,0	44,2	4,2	0,0	0,1	5,1	0,0	0,3	0,2	0,2
0,1	24,8	25,6	37,8	6,0	0,0	0,1	32,7	0,0	0,9	0,6	0,2
0,1	27,5	28,1	37,8	7,8	0,0	0,1	3,5	0,1	0,1	0,1	0,1
0,0	31,2	25,0	31,9	17,7	0,0	0,1	3,2	0,1	0,0	0,1	0,1
0,0	11,6	24,7	43,9	18,7	0,0	0,1	4,4	0,0	0,0	0,2	0,1
0,0	46,2	40,2	20,4	27,4	0,0	0,0	5,6	0,1	0,3	0,2	0,1
0,1	42,2	34,4	17,6	26,0	0,0	0,1	7,4	0,1	0,0	0,3	0,0
0,0	37,9	43,5	9,1	8,6	0,0	19,6	17,0	0,0	0,1	0,3	0,2
0,0	39,2	46,4	12,6	37,2	0,0	22,5	14,7	0,2	0,2	0,2	0,2
0,4	32,8	0,0	0,0	16,6	0,0	5,5	7,3	0,0	0,1	0,1	0,3
0,0	45,1	2,5	0,0	2,8	0,7	0,0	7,3	0,0	0,0	0,2	0,1
0,0	0,1	0,0	0,0	9,3	0,0	0,0	0,0	0,0	0,1	0,1	0,5

Mean	**0,2**	**20,1**	**14,7**	**19,8**	**13,2**	**1,1**	**3,1**	**4,3**	**0,6**	**1,9**	**1,6**	**1,5**
Standard deviation	**0,5**	**16,4**	**14,3**	**18,2**	**8,9**	**3,9**	**6,8**	**6,4**	**2,0**	**4,9**	**4,4**	**4,1**
Median	0,1	18,2	11,6	18,1	10,3	0,0	0,1	2,2	0,1	0,2	0,2	0,2

Fig. 3

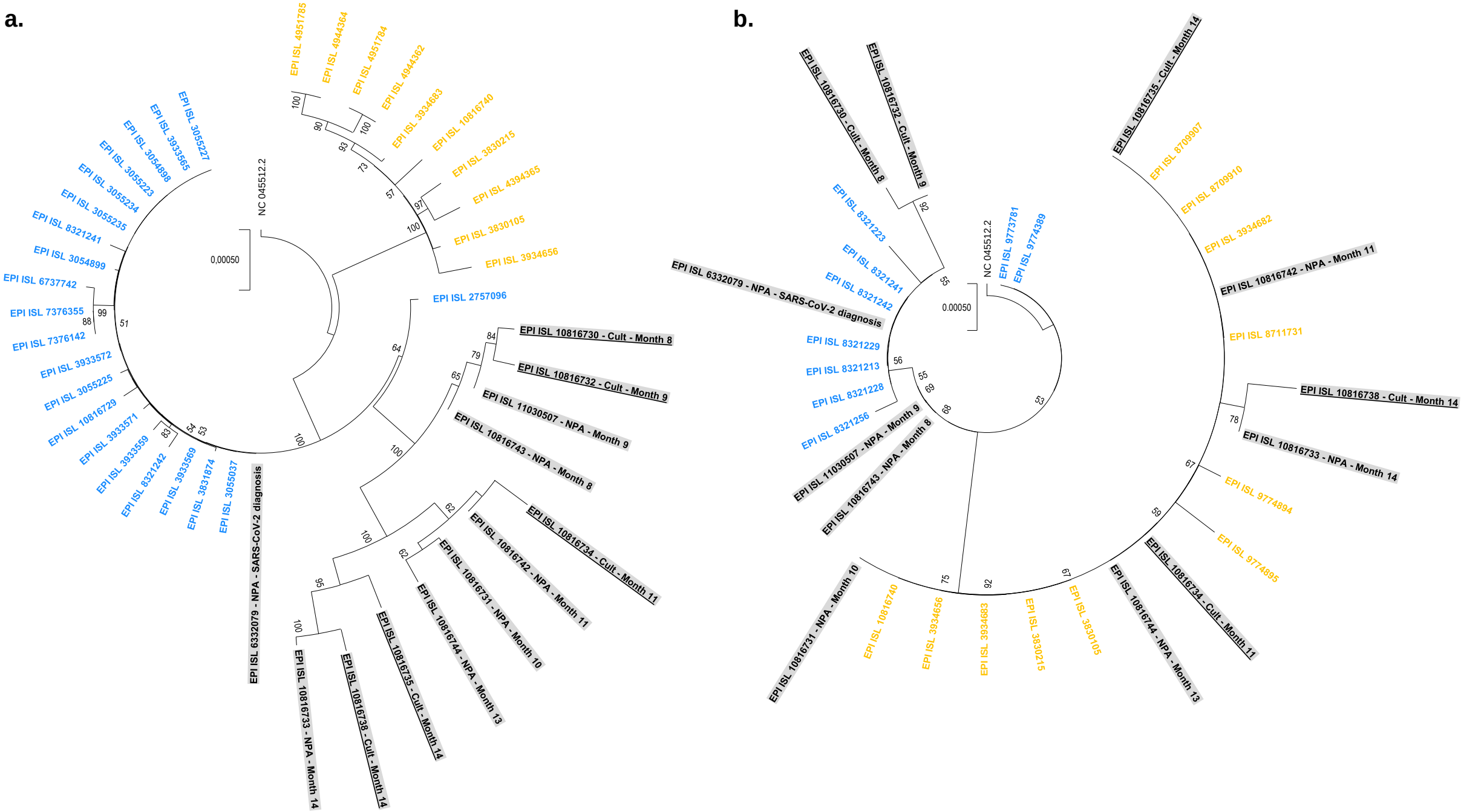
a.
EPI ISL 4951785
EPI ISL 4944364
EPI ISL 4951784
EPI ISL 4944362
EPI ISL 3934683
EPI ISL 10816740
EPI ISL 3830215
EPI ISL 4394365
EPI ISL 3830105
EPI ISL 3934656
EPI ISL 2757096
EPI ISL 10816730 - Cult - Month 8
EPI ISL 10816732 - Cult - Month 9
EPI ISL 11030507 - NPA - Month 9
EPI ISL 10816743 - NPA - Month 8
EPI ISL 10816734 - Cult - Month 11
EPI ISL 10816742 - NPA - Month 11
EPI ISL 10816731 - NPA - Month 10
EPI ISL 10816744 - NPA - Month 13
EPI ISL 10816735 - Cult - Month 14
EPI ISL 10816738 - Cult - Month 14
EPI ISL 10816733 - NPA - Month 14
EPI ISL 6332079 - NPA - SARS-CoV-2 diagnosis
EPI ISL 3055037
EPI ISL 3831874
EPI ISL 3933569
EPI ISL 8321242
EPI ISL 3933559
EPI ISL 3933571
EPI ISL 10816729
EPI ISL 3055225
EPI ISL 3933572
EPI ISL 7376142
EPI ISL 7376355
EPI ISL 6737742
EPI ISL 3054899
EPI ISL 8321241
EPI ISL 3055235
EPI ISL 3055234
EPI ISL 3055223
EPI ISL 3054898
EPI ISL 3933565
EPI ISL 3055227
NC 045512.2
0,00050
b.
EPI ISL 10816730 - Cult - Month 8
EPI ISL 10816732 - Cult - Month 9
EPI ISL 8321223
EPI ISL 8321241
EPI ISL 8321242
EPI ISL 6332079 - NPA - SARS-CoV-2 diagnosis
EPI ISL 8321229
EPI ISL 8321213
EPI ISL 8321228
EPI ISL 8321256
EPI ISL 11030507 - NPA - Month 9
EPI ISL 10816743 - NPA - Month 8
NC 045512.2
EPI ISL 9773781
EPI ISL 9774389
0.00050
EPI ISL 10816731 - NPA - Month 10
EPI ISL 10816740
EPI ISL 3934656
EPI ISL 3934683
EPI ISL 3830215
EPI ISL 3830105
EPI ISL 10816744 - NPA - Month 13
EPI ISL 10816734 - Cult - Month 11
EPI ISL 9774895
EPI ISL 9774894
EPI ISL 10816733 - NPA - Month 14
EPI ISL 10816738 - Cult - Month 14
EPI ISL 8711731
EPI ISL 10816742 - NPA - Month 11
EPI ISL 3934682
EPI ISL 8709910
EPI ISL 8709907
EPI ISL 10816735 - Cult - Month 14

SUPPLEMENTARY MATERIAL

Full-length title:

Sequential appearance and isolation of a SARS-CoV-2 recombinant between two major SARS-CoV-2 variants in a chronically infected immunocompromised patient

SUPPLEMENTARY METHODS

At our institute, SARS-CoV-2 real-time reverse-transcription-PCR (qPCR) was performed on nasopharyngeal samples collected from patients tested by real-time reverse-transcription-PCR (qPCR) using the BGI real-time fluorescent RT-PCR assay (BGI Genomics, Shanghai Fosun Long March Medical Science Co., Ltd., Shenzhen, China) or the NeuMoDx SARS-CoV-2 assay (NeuMoDx Molecular, Ann Arbor, Michigan). Outside our institute (medical biology laboratory Alphabio, hôpital Européen, France), SARS-CoV-2 qPCR was performed using the BD MAX System (Becton Dickinson, Sparks, MD, USA).

SUPPLEMENTARY RESULTS

Virological follow-up by SARS-CoV-2 real-time reverse-transcription-PCR (qPCR)

SARS-CoV-2 qPCR performed on nasopharyngeal samples was positive between summer 2020 (at time of SARS-CoV-2 diagnosis) and Month 4 post-diagnosis, then negative once at Month 5 but positive again on the next sample tested in Month 7. Between Month 8 and Month 11, qPCR remained almost always positive being only transiently negative for ≤3 days. Then qPCR was consistently positive when performed between Month 13 and Month 14 post-diagnosis.

Nucleotide diversity at positions harboring signature mutations of the B.1.160 or Alpha variants

Regarding the SARS-CoV-2 genomes obtained from the respiratory samples, which

were obtained with the Illumina technology except for the sample collected at Month 11 post-SARS-CoV-2 diagnosis for which the genome was obtained with the Nanopore technology, nucleotide di-versity at the 35 positions harboring signature mutations of the B.1.160 or Alpha variants differed according to the time of sample collection. It was low at time of diagnosis in 2020, with a mean (±standard deviation) value of 0.2±0.5%, increased to reach high values at Month 8 (20.1±16.4%), at Month 9 (14.7±14.3%), at Month 10 (19.8±18.2%), and at Month 11 (13.2±8.9%), then decreased to low values again at Month 13 (1.1±3.9%) and at Month 14 (3.1±6.8%) (Figure 2 of the main text). The low nucleotide diversity observed for genomes obtained at Month 13 and at Month 14 indicated that the mosaicism consisting in the presence of signature mutations of the two variants was not explained by a co-infection by these two variants or by a contamination of the samples prior or during the next-generation sequencing procedure.

Regarding the genomes obtained from the culture supernatants, which were all ob-tained with the Illumina technology, nucleotide diversity at positions harboring signature mutations of the B.1.160 or Alpha variants was low, indicating that these genomes, including those recombinants, were generated from a single viral isolate. Indeed, mean nucleotide diversity ranged between 0.6±2.0% and 4.3±6.4% (Figure 2 of the main text). The viral genomes obtained from the culture of the respiratory samples collected at Month 14 were highly similar to the viral genome obtained directly from the respiratory sample collected at Month 14.

Generation of additional sequence reads

Sequencing of reverse-transcription-PCR-targeted regions: We attempted to generate sequence reads that are hybrids of the B.1.160 and Alpha variants from the respiratory sample collected at Month 11 by PCR amplification of the regions overlapping re-combination sites then next-generation sequencing with the Oxford Nanopore Technol-ogy (ONT) on a GridION instrument (Oxford Nanopore Technologies Ltd., Oxford, United Kingdom).

Amplicons corresponding to positions 3,100-4,570 (in reference to the genome of the Wuhan-Hu-1 isolate GenBank accession no. NC_045512.2) were amplified using the following primers (in 5'-3' orientation): Forward: TTCAACCTGAAGAA-GAGCAA; reverse: TGGCATTGTAACAAGAGTTT. Amplicons corresponding to posi-tions 24,813-29,074 were amplified using the following primers: Forward: ATGGAAAAGCACACTTTCCT; reverse: GCTTTAGTGGCAGTACGTTT. For the am-plicons corresponding to positions 3,100-4,570, 87% of the reads were hybrids harboring both Alpha (C3267U) and B.1.160 (C4543U) signature mutations. For the amplicon cor-responding to positions 24,813-29,074, 70% of the reads were hybrids harboring Alpha (G24914C) and B.1.160 (G25563U, C25710U, C26735U, U26876C and G28975C) mutations, and 24% were hybrids harboring Alpha mutation G24914C and B.1.160 mutation G28975C.

Metagenomic sequencing: Next-generation sequencing was also carried out using a metagenomic approach with the Nanopore technology on a GridION instrument (Oxford Nanopore Technologies Ltd.) to attempt obtaining long sequence reads and detect addi-tional reads that are hybrids of the B.1.160 and Alpha variants. For the first recombination site, four reads with a length ranging between 1,855-11,979 nucleotides were obtained, which harbored signature mutations of the Alpha (C3267U) and B.1.160 (C4543U) variants. For the third recombination site, four reads with a length comprised between 1,486-8,143 nucleotides were obtained that harbored signature mutations of the Alpha (G24914C) and B.1.160 (C25563U) variants.

Viral culture

Cytopathic effects were observed between 4 and 8 days after the inoculation of the nasopharyngeal samples on Vero E6 cells as previously described [1] (Table 2 of the main text).

Phylogenetic analyses based on SARS-CoV-2 genomes and spike gene sequences

Phylogeny reconstructions were performed based on viral genomes or spike genes, which included sequences obtained directly from the nasopharyngeal samples and from the cultures, and their best BLAST hits from the IHU Méditerranée Infection sequence database that were classified as B.1.160 or Alpha variants [2]. The genome obtained from the nasopharyngeal sample collected in 2020 at time of SARS-CoV-2 diagnosis was clustered with genomes of the B.1.160 variant, apart from the other genomes obtained from the case-patient (Figure 3a of the main text). Other genomes obtained from the nasopharyngeal samples collected since Month 8 and those obtained from cultures of the nasopharyngeal samples collected since Month 8 were also clustered with genomes of the B.1.160 variant, but they were clustered together, apart from the other genomes. The Alpha variant genomes were clustered apart from all other genomes. Spike gene phylogeny showed the clusterisation with sequences of the B.1.160 variant of the sequences obtained from the case-patient either directly or post-culture from samples collected between SARS-CoV-2 diagnosis and Month 9 post-diagnosis (Figure 3b of the main text). In contrast, sequences obtained from the case-patient either directly or post-culture from samples collected since Month 10 post-diagnosis were clustered with Alpha variant sequences.

SUPPLEMENTARY FIGURES

Supplementary Figure S1. Majority nucleotides and nucleotide diversity for sequences obtained from the respiratory samples and the culture supernatant at nucleotide positions of the SARS-CoV-2 genome that harbor signature mutations of the B.1.160 or Alpha variants and at any other positions that harbor mutations.

Nucleotide positions are in reference to the genome of the Wuhan-Hu-1 isolate GenBank accession no. NC_045512.2. B.1.160 nucleotides are indicated by a blue background; Alpha nucleotides are indicated by a yellow background. Del, nucleotide deletion. Nucleotide

101 diversity is the proportion of sequence reads that do not harbor the consensus (majority)

102 nucleotide.

103

Nucleotide positions	Wuhan-Hu-1 isolate genome	Signature mutations in B.1.160/Marseille-4 genomes	Signature mutations in Alpha genomes	Majority nucleotides: Nasopharyngeal samples: SARS-CoV-2 diagnosis	Majority nucleotides: Nasopharyngeal samples: Month 8	Majority nucleotides: Nasopharyngeal samples: Month 9	Majority nucleotides: Nasopharyngeal samples: Month 10	Majority nucleotides: Nasopharyngeal samples: Month 11	Majority nucleotides: Nasopharyngeal samples: Month 13	Majority nucleotides: Nasopharyngeal samples: Month 14	Majority nucleotides: Culture supernatants: Month 8	Majority nucleotides: Culture supernatants: Month 9	Majority nucleotides: Culture supernatants: Month 11	Majority nucleotides: Culture supernatants: Month 14	Majority nucleotides: Culture supernatants: December 2nd, 2021	Nucleotide diversity (%): Nasopharyngeal samples: SARS-CoV-2 diagnosis	Nucleotide diversity (%): Nasopharyngeal samples: Month 8	Nucleotide diversity (%): Nasopharyngeal samples: Month 9	Nucleotide diversity (%): Nasopharyngeal samples: Month 10	Nucleotide diversity (%): Nasopharyngeal samples: Month 11	Nucleotide diversity (%): Nasopharyngeal samples: Month 13	Nucleotide diversity (%): Nasopharyngeal samples: Month 14	Nucleotide diversity (%): Culture supernatants: Month 8	Nucleotide diversity (%): Culture supernatants: Month 9	Nucleotide diversity (%): Culture supernatants: Month 11	Nucleotide diversity (%): Culture supernatants: Month 14	Nucleotide diversity (%): Culture supernatants: Month 14
7	G	-	-	-	-	-	U	-	-	-	-	-	-	-	-	0,0	0,0	0,0	0,0	0,0	0,0	0,0	16,7	0,0	0,0	0,0	/
241	C	U	U	U	U	U	U	U	U	U	U	U	U	U	U	0,0	0,0	0,0	0,1	10,6	0,0	0,1	0,0	0,1	0,0	0,0	0,4
629	C	-	-	-	U	U	U	U	U	U	-	-	U	U	U	0,2	45,5	13,2	25,1	28,4	0,1	1,0	6,4	0,1	0,2	0,1	0,3
696	A	-	-	-	-	-	U	U	U	U	-	-	U	U	U	0,0	37,5	29,6	32,0	4,5	0,2	0,1	4,9	0,0	0,1	0,5	0,2
913	C	-	U	-	-	-	U	U	U	U	-	-	U	U	U	0,0	33,9	26,8	35,9	10,0	0,1	0,1	9,0	0,1	0,1	0,1	0,3
981	C	-	-	-	-	-	-	-	-	U	-	-	-	-	-	0,0	0,0	0,1	0,0	4,0	0,0	14,0	0,0	0,2	0,1	0,4	0,4
1192	A	-	-	-	-	-	-	-	G	-	-	-	-	-	-	0,2	0,0	0,1	0,2	2,6	33,3	0,0	0,0	0,0	0,1	0,1	0,1
1677	A	-	-	-	-	-	-	-	-	-	-	-	-	C	-	0,0	0,0	0,0	0,0	2,3	0,0	15,0	0,1	0,1	0,1	0,3	0,0
1683	U	-	-	-	-	-	-	-	-	C	-	-	-	-	C	0,0	0,0	0,0	0,0	1,4	0,0	18,5	0,1	0,1	0,0	0,1	0,1
1895	G	-	-	-	-	-	-	-	A	-	-	-	-	-	-	0,5	0,0	0,0	0,0	6,4	0,0	0,0	0,0	0,0	0,5	0,0	0,3
1978	U	-	-	-	-	-	-	-	C	-	-	-	-	-	-	0,1	0,0	0,0	0,0	1,0	12,7	0,2	0,1	0,2	0,0	0,2	0,3
2509	C	-	-	-	-	-	-	-	-	-	-	-	-	U	-	0,5	0,0	0,0	0,0	3,4	0,0	7,4	0,0	0,0	0,0	0,8	0,0
2594	C	-	-	-	-	-	-	-	-	U	-	-	-	U	U	0,0	0,0	0,0	0,0	2,2	0,0	0,0	0,1	0,0	0,0	0,1	0,2
2706	C	-	-	-	U	U	-	-	-	U	U	U	-	U	U	0,1	43,6	25,0	28,1	5,4	0,0	0,1	4,3	0,1	0,0	0,2	0,0
3037	C	U	U	U	U	U	U	U	U	U	U	U	U	U	U	0,3	0,3	1,3	0,0	20,8	0,0	0,1	0,0	0,1	0,0	0,4	0,1
3193	A	-	-	-	-	-	G	G	G	-	-	-	G	-	-	0,3	0,0	25,5	33,4	21,2	0,9	0,0	0,0	0,0	2,6	0,0	0,6
3224	A	-	-	-	-	-	-	-	G	-	-	-	-	-	-	0,0	0,0	0,0	0,0	6,3	0,1	0,1	0,0	0,0	0,0	0,0	0,0
3267	C	-	U	-	-	-	U	U	U	-	-	-	U	-	-	0,0	28,8	23,7	39,3	6,8	0,0	0,0	2,4	0,1	0,2	0,4	0,1
3340	G	-	-	-	-	-	-	-	-	-	-	-	-	U	-	0,0	16,8	0,0	0,0	2,3	0,1	12,7	0,1	0,1	0,0	0,0	0,3
3393	C	-	-	-	-	U	-	-	-	-	U	U	-	-	-	0,3	28,7	43,4	20,8	4,6	0,0	0,2	2,4	0,0	0,0	0,0	0,1
4543	C	U	-	U	U	U	U	U	U	U	U	U	U	U	U	0,1	0,0	0,0	0,0	7,8	0,0	0,1	0,3	0,2	0,2	0,8	0,1
4872	A	-	-	-	G	G	-	-	-	-	G	G	-	-	-	0,1	0,0	12,5	37,1	2,9	0,0	0,0	0,0	0,1	0,0	0,1	0,1
4878	C	-	-	-	U	U	U	U	U	U	U	U	U	U	U	0,0	0,0	0,0	0,0	6,6	0,0	0,2	0,1	0,1	0,1	0,2	0,2
4893	C	-	-	-	-	-	U	U	U	U	-	-	U	U	U	0,1	0,0	27,3	43,3	5,2	0,6	0,0	0,1	0,0	0,2	0,1	0,2
4904	G	-	-	-	-	A	-	-	-	-	A	A	-	-	-	0,0	10,5	30,0	47,9	1,7	0,0	0,0	4,8	0,0	0,0	0,2	0,1
5278	U	-	-	-	-	-	-	-	-	-	-	-	-	C	-	0,9	0,0	0,0	0,0	2,1	0,0	14,6	0,0	0,0	0,0	8,0	0,0
5629	G	U	-	U	U	U	U	U	U	U	U	U	U	U	U	2,8	0,5	1,6	0,2	11,4	0,6	0,0	0,8	1,9	0,9	5,3	1,5
5648	A	-	-	-	-	-	-	-	-	C	-	-	-	C	C	0,1	0,1	0,0	0,0	1,6	0,0	0,1	0,1	0,0	0,0	0,2	0,1
5986	C	-	U	-	-	-	-	-	-	-	-	-	U	-	-	0,0	0,0	0,0	0,0	10,3	0,0	0,0	0,0	0,0	18,4	0,0	0,1
6629	C	-	-	-	-	U	-	-	-	-	-	U	-	-	-	0,0	0,0	37,7	15,6	5,6	0,0	0,0	0,0	0,3	0,3	0,1	0,1
6633	C	-	-	-	U	U	U	U	U	U	U	U	U	U	U	0,0	0,2	0,0	0,0	11,0	0,1	0,0	0,0	0,1	0,3	0,1	0,2
7113	C	-	-	-	-	-	-	-	-	U	-	-	-	-	U	0,0	0,0	/	0,0	3,4	0,0	15,5	0,0	0,0	0,0	0,3	1,5
7185	U	-	-	-	C	C	C	C	C	C	C	C	C	C	C	0,1	0,0	0,0	0,0	10,9	0,0	0,0	0,1	0,0	0,0	0,4	0,1
7279	C	-	-	-	-	-	-	-	-	U	-	-	-	-	-	0,1	0,0	0,0	2,7	2,5	0,0	31,3	0,2	0,3	0,5	0,3	0,5
8191	U	-	-	-	-	-	-	-	-	-	-	-	A	-	-	0,1	0,0	0,0	0,0	12,0	0,2	0,2	0,1	0,0	16,0	0,2	0,0
8770	C	-	-	-	U	-	-	-	-	-	-	-	-	-	-	0,0	47,2	0,0	0,0	10,6	0,0	0,1	3,1	0,1	0,0	0,7	0,1
8950	C	-	-	-	-	-	-	-	-	-	-	U	-	-	-	0,1	0,0	48,1	14,9	1,6	0,1	0,1	0,2	0,1	0,1	0,2	0,1
9042	C	-	-	-	U	U	U	U	U	U	U	U	U	U	U	0,0	0,1	0,1	0,2	17,7	0,0	0,1	0,1	0,5	0,1	0,1	0,3
9120	C	-	-	-	U	U	U	U	U	U	U	U	U	U	U	0,0	0,0	0,0	0,0	8,6	0,0	0,3	0,0	0,0	0,1	0,2	0,3
9501	C	-	-	-	U	-	U	U	U	U	U	U	U	U	U	0,0	0,0	/	0,0	9,1	0,0	0,0	0,6	2,6	0,4	0,5	2,2
9526	G	U	-	U	U	U	U	U	U	U	U	U	U	U	U	0,1	0,0	0,0	0,0	4,6	0,0	0,8	1,2	0,2	0,2	0,0	0,3
9626	U	-	-	-	C	-	-	-	-	-	-	-	-	-	-	0,0	50,0	/	0,0	15,5	0,0	0,0	0,3	0,1	0,0	0,0	0,5
9783	G	-	-	-	-	-	-	C	-	-	-	-	-	-	-	0,0	0,0	/	0,0	35,0	0,0	0,0	0,0	0,0	0,0	0,0	0,2
9792	A	-	-	-	-	C	-	-	-	-	-	-	-	-	-	0,0	16,7	0,0	0,0	2,2	0,0	0,0	1,2	0,0	0,0	0,0	0,0
9811	C	-	-	-	-	-	-	-	-	U	-	-	-	U	U	0,1	0,0	0,0	0,0	6,1	0,0	2,9	0,0	0,1	0,2	0,7	0,6
9972	A	-	-	-	-	-	-	-	-	G	-	-	-	-	-	0,0	0,0	0,0	0,0	5,7	0,0	21,6	0,0	0,0	0,2	0,0	0,1
11083	G	-	-	-	-	-	-	-	-	-	U	-	-	-	-	1,0	1,1	0,0	0,0	2,2	0,0	0,7	27,1	0,1	0,1	0,7	0,5
11208	C	-	-	-	U	U	U	U	U	U	U	U	U	U	U	0,0	0,0	0,2	0,1	4,6	0,2	0,0	0,2	0,1	0,0	0,2	0,1
11365	G	-	-	-	-	-	-	-	-	U	-	-	-	-	U	0,0	0,0	0,0	0,0	2,3	0,0	19,2	0,1	0,0	0,0	0,1	0,1
11497	C	U	-	U	U	U	U	U	U	U	U	U	U	U	U	0,4	0,0	0,0	0,3	2,5	0,4	0,0	0,1	0,3	0,2	0,1	0,2
12459	C	-	-	-	-	U	-	-	-	-	-	U	-	-	-	0,4	0,0	45,8	20,6	3,1	0,0	0,1	0,3	0,1	0,4	0,2	0,3
12592	U	-	-	-	-	C	-	-	-	-	-	C	-	-	-	0,0	0,2	39,0	23,5	2,1	0,0	0,0	0,1	0,1	0,0	0,1	0,1
13506	C	-	-	-	U	U	U	U	U	U	U	U	U	U	U	0,0	0,0	0,0	0,0	13,9	0,0	0,0	0,0	0,1	0,0	0,1	0,1
13517	C	-	-	-	-	-	-	-	U	-	-	-	-	-	-	0,3	0,0	0,0	0,0	3,6	16,7	0,1	0,4	0,1	0,6	0,1	0,2
13860	C	-	-	-	-	-	U	U	U	-	-	-	U	-	-	0,2	0,1	24,2	35,4	3,9	0,1	0,1	0,1	0,2	0,0	0,1	0,2
13936	G	-	-	-	-	-	-	-	-	-	-	-	-	-	U	0,0	0,0	0,1	0,0	4,3	0,3	0,0	0,1	0,0	0,0	0,1	3,0
13993	G	U	-	U	U	U	U	U	U	U	U	U	U	U	U	0,1	0,1	0,0	0,1	5,4	0,1	0,0	0,0	0,1	0,0	0,3	0,1
14408	C	U	U	U	U	U	U	U	U	U	U	U	U	U	U	0,1	0,1	0,0	0,1	11,0	0,1	0,4	0,1	0,3	0,0	0,3	0,2
15766	G	U	-	U	U	U	U	U	U	U	U	U	U	U	U	0,1	0,3	0,0	0,1	9,2	0,0	0,0	0,0	0,1	0,0	0,1	0,1
16128	A	-	-	-	-	-	-	-	-	-	-	-	-	G	-	0,2	0,0	0,1	0,1	2,3	0,0	13,9	0,0	0,0	0,0	12,1	0,0
16675	C	-	-	-	U	U	U	U	U	U	U	U	U	U	U	0,1	0,2	0,0	0,2	13,2	0,1	0,0	0,1	0,7	0,5	0,2	0,1
16751	C	-	-	-	U	U	U	U	U	U	U	U	U	U	U	7,0	0,0	0,0	0,2	11,2	0,4	0,6	0,3	0,9	0,0	0,6	0,0
16889	A	G	-	G	G	G	G	G	G	G	G	G	G	G	G	0,1	0,0	0,0	0,0	7,7	0,0	0,2	0,0	0,1	0,0	0,3	0,1
17019	G	U	-	U	U	U	U	U	U	U	U	U	U	U	U	0,0	0,0	0,0	0,0	15,6	0,0	0,0	0,3	0,2	0,4	0,1	0,1
17122	G	-	-	-	-	-	-	-	-	U	-	-	-	-	U	0,1	0,0	0,0	0,0	11,9	0,1	16,0	0,0	0,1	0,1	0,1	0,1
17125	C	-	-	-	-	-	U	U	U	-	-	-	U	-	-	0,1	0,0	18,9	43,4	18,4	0,1	0,0	0,1	0,0	0,1	0,2	0,2
17251	C	-	-	-	U	U	U	U	U	U	U	U	U	U	U	0,0	0,3	0,1	0,1	11,1	0,2	0,1	0,2	0,1	0,1	0,5	0,5

104

105 *Supplementary Figure S2 (continued)*

Nucleotide positions	Wuhan-Hu-1 isolate genome	Signature mutations in B.1.160/Marseille-4 genomes	Signature mutations in Alpha genomes	Majority nucleotides: Nasopharyngeal samples: SARS-CoV-2 diagnosis	Majority nucleotides: Nasopharyngeal samples: Month 8	Majority nucleotides: Nasopharyngeal samples: Month 9	Majority nucleotides: Nasopharyngeal samples: Month 10	Majority nucleotides: Nasopharyngeal samples: Month 11	Majority nucleotides: Nasopharyngeal samples: Month 13	Majority nucleotides: Nasopharyngeal samples: Month 14	Majority nucleotides: Culture supernatants: Month 8	Majority nucleotides: Culture supernatants: Month 9	Majority nucleotides: Culture supernatants: Month 11	Majority nucleotides: Culture supernatants: Month 14	Majority nucleotides: Culture supernatants: December 2nd, 2021	Nucleotide diversity (%): Nasopharyngeal samples: SARS-CoV-2 diagnosis	Nucleotide diversity (%): Nasopharyngeal samples: Month 8	Nucleotide diversity (%): Nasopharyngeal samples: Month 9	Nucleotide diversity (%): Nasopharyngeal samples: Month 10	Nucleotide diversity (%): Nasopharyngeal samples: Month 11	Nucleotide diversity (%): Nasopharyngeal samples: Month 13	Nucleotide diversity (%): Nasopharyngeal samples: Month 14	Nucleotide diversity (%): Culture supernatants: Month 8	Nucleotide diversity (%): Culture supernatants: Month 9	Nucleotide diversity (%): Culture supernatants: Month 11	Nucleotide diversity (%): Culture supernatants: Month 14	Nucleotide diversity (%): Culture supernatants: Month 14
17721	G	-	-	-	-	-	-	-	-	-	-	-	U	-	0,1	0,0	0,0	0,0	5,0	0,0	11,7	0,1	0,1	0,1	0,2	0,3
17738	C	-	-	-	-	-	-	-	U	-	-	-	-	-	0,0	0,0	0,0	0,1	9,3	1,0	0,0	0,1	0,1	0,1	0,2	0,1
18023	A	-	-	-	-	-	-	-	-	G	-	-	-	-	0,0	0,2	0,1	0,1	0,9	0,2	22,3	0,2	0,0	0,1	0,5	0,4
18877	C	U	-	U	-	U	U	U	U	-	U	U	U	-	0,0	47,0	0,0	0,0	6,8	0,0	0,1	2,7	0,2	0,0	0,2	0,1
19186	C	-	-	-	-	-	-	-	-	-	-	-	-	-	0,1	0,1	0,1	0,0	4,5	0,0	0,5	0,3	0,0	0,2	44,5	0,1
19383	U	-	-	-	-	-	-	C	-	-	-	-	-	-	0,0	0,0	0,0	0,0	0,0	0,0	0,0	0,0	0,0	0,0	0,2	0,2
19439	C	-	-	-	-	-	-	A	-	-	-	-	-	-	0,1	0,0	0,0	0,0	50,0	0,4	0,5	0,1	0,2	0,0	0,1	0,2
19456	U	-	-	-	-	-	-	C	-	-	-	-	-	-	0,0	0,0	0,0	0,0	50,0	0,0	0,2	0,0	0,0	0,1	0,0	0,4
19473	U	-	-	-	-	-	-	C	-	-	-	-	-	-	0,1	0,0	1,2	0,0	50,0	0,0	0,2	0,1	0,1	0,3	0,2	0,2
19547	C	-	-	-	-	-	-	-	-	-	-	-	U	-	0,0	0,0	0,0	0,0	4,9	0,0	0,0	0,0	0,0	15,2	0,1	0,3
19947	G	-	-	-	-	-	-	U	-	-	-	-	-	-	0,0	0,0	0,0	0,0	59,4	0,0	0,2	0,0	0,2	0,0	0,4	0,1
20930	C	-	-	-	-	-	-	-	-	-	U	-	-	-	0,1	18,5	0,0	0,0	5,8	0,1	0,0	6,2	0,1	0,0	0,2	0,1
21219	C	-	-	-	-	-	-	-	-	U	-	-	-	-	0,0	0,0	0,0	0,0	0,0	0,0	30,1	0,1	0,0	0,0	0,2	0,1
21232	G	-	-	-	-	-	-	-	-	-	-	-	-	U	0,1	0,0	0,0	0,0	0,0	0,0	19,3	0,0	0,1	0,0	0,3	0,3
21575	C	-	-	-	-	U	-	-	-	-	U	U	-	-	1,2	44,4	42,4	14,4	8,2	0,0	0,5	4,4	1,2	5,4	0,1	0,5
21765	U	-	Del	-	-	-	-	Del	Del	Del	-	-	Del	Del	Del	0,1	14,7	11,0	38,3	39,2	22,6	22,9	2,1	0,0	21,8	23,7	21,2
21766	A	-	Del	-	-	-	-	Del	Del	Del	-	-	Del	Del	Del	0,0	16,2	11,8	44,0	10,9	1,6	1,1	2,2	0,0	1,2	1,6	1,0
21767	C	-	Del	-	-	-	-	Del	Del	Del	-	-	Del	Del	Del	0,1	15,4	11,1	42,8	19,6	0,0	0,0	2,1	0,0	0,0	0,1	0,0
21768	A	-	Del	-	-	-	-	Del	Del	Del	-	-	Del	Del	Del	0,0	15,4	11,2	43,1	10,4	0,0	0,0	2,1	0,0	0,0	0,1	0,1
21769	U	-	Del	-	-	-	-	Del	Del	Del	-	-	Del	Del	Del	0,0	15,6	11,5	43,7	13,7	0,2	0,2	2,1	0,1	0,2	0,5	0,5
21770	G	-	Del	-	-	-	-	Del	Del	Del	-	-	Del	Del	Del	0,1	18,2	15,2	47,6	9,6	5,6	5,6	3,6	0,0	7,2	6,4	6,5
21991	U	-	Del	-	-	Del	Del	Del	Del	Del	-	Del	Del	Del	Del	0,0	20,3	17,3	18,6	22,1	1,3	4,3	0,1	2,1	2,5	0,7	1,4
21992	U	-	Del	-	-	Del	Del	Del	Del	Del	-	Del	Del	Del	Del	0,1	20,4	16,9	18,1	20,3	1,3	5,6	0,1	2,1	2,5	2,0	2,1
21993	A	-	Del	-	-	Del	Del	Del	Del	Del	-	Del	Del	Del	Del	0,1	20,6	16,7	17,7	17,8	3,7	18,9	0,1	11,5	7,4	10,7	12,6
22992	G	A	-	A	A	/	-	-	-	-	A	A	-	-	-	0,3	33,3	/	20,6	4,8	0,0	0,0	5,5	0,1	0,0	0,2	0,3
23063	A	-	U	-	-	-	U	U	U	U	-	-	U	U	U	0,0	50,0	33,3	27,1	12,4	0,0	0,0	6,7	0,1	0,0	0,4	0,4
23188	C	-	-	-	-	-	-	-	-	-	U	-	-	-	-	0,0	0,0	0,0	0,0	2,3	0,0	0,1	7,3	0,0	0,1	0,2	0,1
23271	C	-	A	-	-	-	A	A	A	A	-	-	A	A	A	0,2	15,7	20,0	44,2	4,2	0,0	0,1	5,1	0,0	0,3	0,2	0,2
23277	C	-	-	-	-	-	-	-	-	-	-	-	-	-	U	0,0	0,0	0,0	0,0	7,9	0,0	0,2	0,2	0,0	0,2	0,1	0,3
23403	A	G	G	G	G	G	G	G	G	G	G	G	G	G	G	0,2	0,0	0,0	0,0	17,4	0,1	0,0	0,1	0,1	0,0	0,1	0,2
23415	C	-	-	-	-	-	-	-	-	A	-	-	-	-	A	0,1	0,0	0,0	0,0	3,6	1,3	14,0	0,2	0,0	0,1	0,1	0,2
23525	C	-	-	-	-	-	-	-	-	-	-	-	-	-	U	0,0	0,0	0,0	0,0	2,4	0,0	0,0	0,1	0,1	0,0	0,2	0,2
23598	A	-	-	-	-	-	-	-	-	-	G	-	-	-	-	0,1	0,0	0,1	0,0	1,6	0,0	0,1	49,0	0,1	0,8	0,4	0,0
23604	C	-	A	-	-	-	A	A	A	A	A	-	A	A	A	0,1	24,8	25,6	37,8	6,0	0,0	0,1	32,7	0,0	0,9	0,6	0,2
23709	C	-	U	-	-	-	U	U	U	U	-	-	U	U	U	0,1	27,5	28,1	37,8	7,8	0,0	0,1	3,5	0,1	0,1	0,1	0,1
23948	G	-	-	-	C	C	-	-	-	-	C	C	-	-	-	0,0	36,9	37,9	29,0	2,2	0,0	0,2	4,1	0,0	0,0	0,3	0,4
24023	C	-	-	-	U	U	-	-	-	-	U	U	-	-	-	0,0	43,5	43,5	27,4	2,0	0,0	0,4	5,7	0,3	0,2	0,2	0,7
24506	U	-	G	-	-	-	G	G	G	G	-	-	G	G	G	0,0	31,2	25,0	31,9	17,7	0,0	0,1	3,2	0,1	0,0	0,1	0,1
24914	G	-	C	-	-	-	C	C	C	C	-	-	C	C	C	0,0	11,6	24,7	43,9	18,7	0,0	0,1	4,4	0,0	0,0	0,2	0,1
25460	C	-	-	-	-	-	-	U	-	-	-	-	U	-	-	0,2	0,1	49,6	12,9	26,2	0,0	0,3	0,2	0,3	0,1	0,2	0,1
25515	C	-	-	-	-	-	A	-	A	-	-	-	-	-	-	0,0	0,0	29,4	31,9	37,6	0,1	0,3	0,0	0,0	0,1	0,2	0,2
25517	C	-	-	-	-	-	-	-	-	U	-	-	-	-	-	0,1	0,0	0,0	0,1	9,9	0,0	37,0	0,1	0,0	0,2	0,1	0,1
25521	C	-	-	-	-	-	-	-	-	-	-	-	-	U	-	0,1	0,1	0,0	0,1	3,1	0,1	27,9	0,2	0,1	0,1	0,9	0,0
25563	G	U	-	U	U	U	-	U	-	-	U	U	U	-	-	0,0	46,2	40,2	20,4	27,4	0,0	0,0	5,6	0,1	0,3	0,2	0,1
25710	C	U	-	U	-	U	-	U	-	-	U	U	U	-	-	0,1	42,2	34,4	17,6	26,0	0,0	0,1	7,4	0,1	0,0	0,3	0,0
26204	C	-	-	-	-	-	-	U	-	-	U	-	U	-	-	0,0	23,5	42,9	25,9	28,1	0,0	0,0	3,7	23,0	10,6	0,0	0,0
26681	C	-	-	-	-	-	-	-	U	-	-	-	-	-	-	3,1	0,1	0,0	0,1	6,2	49,1	0,3	0,2	0,1	0,1	0,0	0,2
26735	C	U	-	U	-	-	-	-	-	-	U	U	U	U	-	0,0	37,9	43,5	9,1	8,6	0,0	19,6	17,0	0,0	0,1	0,3	0,2
26819	U	-	-	-	-	-	-	G	-	-	-	-	-	-	-	0,1	0,0	0,0	0,0	35,4	0,1	0,0	0,0	0,1	0,0	0,1	0,3
26835	C	-	-	-	-	-	-	U	-	-	-	-	-	-	-	0,0	0,0	0,0	0,1	45,4	0,0	0,0	0,1	0,0	0,0	0,2	0,1
26858	C	-	-	-	U	-	U	-	U	U	-	-	-	-	U	0,0	44,1	48,8	13,5	23,6	0,0	28,6	20,2	0,0	0,0	0,1	0,1
26876	U	C	-	C	-	-	-	C	-	-	C	C	C	C	-	0,0	39,2	46,4	12,6	37,2	0,0	22,5	14,7	0,2	0,2	0,2	0,2
26907	C	-	-	-	-	-	-	U	-	-	U	U	U	-	-	0,0	24,9	48,8	43,7	34,9	0,0	0,0	49,1	21,2	15,8	0,6	0,0
26952	A	-	-	-	-	-	-	-	-	-	-	-	-	G	-	0,0	0,0	0,0	0,0	1,5	0,0	28,3	0,0	0,0	0,0	0,1	0,1
27459	G	-	-	-	-	-	-	-	-	U	-	-	-	-	U	0,0	0,0	0,0	0,1	10,0	0,6	11,1	0,1	0,0	0,0	0,0	2,3
27918	A	-	-	-	-	-	-	-	G	G	-	-	-	G	G	0,3	0,0	0,3	5,1	21,8	0,0	0,0	0,0	0,1	0,0	0,0	0,0
28038	G	-	-	-	-	-	-	-	U	U	-	-	-	U	U	0,0	0,0	1,5	6,4	26,7	0,0	0,0	0,1	0,0	0,1	0,0	0,0
28271	A	-	-	-	U	U	U	U	U	U	U	U	U	U	U	0,1	35,5	0,1	0,0	11,4	0,0	0,1	6,2	0,1	0,3	0,3	0,1
28338	A	-	-	-	-	-	-	-	-	-	-	-	-	-	G	0,1	0,0	0,0	0,0	1,3	0,0	0,0	0,0	0,0	0,0	0,1	0,3
28560	G	-	-	-	U	U	U	U	U	C	U	U	U	U	C	0,1	0,0	0,0	0,1	4,4	0,1	19,2	0,0	0,0	0,0	0,3	0,1
28572	A	-	-	-	-	-	-	-	-	G	-	-	-	-	G	0,1	0,0	0,0	0,1	1,2	0,0	21,0	0,0	0,0	0,0	0,1	0,2
28657	C	-	-	-	-	-	-	-	-	-	-	-	-	-	U	0,2	0,0	0,0	0,0	2,5	0,0	0,6	0,1	0,0	0,0	0,1	0,3
28887	C	-	-	-	-	-	-	-	-	U	-	-	-	-	U	0,2	0,0	0,0	0,0	3,5	0,0	15,5	0,2	0,1	0,1	0,4	0,0
28975	G	C	-	C	-	C	C	C	C	C	C	C	C	C	C	0,4	32,8	0,0	0,0	16,6	0,0	5,5	7,3	0,0	0,1	0,1	0,3
28977	C	-	U	-	U	-	-	-	-	-	-	-	-	-	-	0,0	45,1	2,5	0,0	2,8	0,7	0,0	7,3	0,0	0,0	0,2	0,1
29242	A	-	-	-	U	-	-	-	-	-	-	-	-	-	-	0,1	47,9	0,2	0,1	2,0	0,0	0,1	5,8	0,0	0,2	0,3	0,3
29399	G	A	-	A	A	A	A	A	A	A	A	A	A	A	A	0,0	0,1	0,0	0,0	9,3	0,0	0,0	0,0	0,0	0,1	0,1	0,5
29445	C	-	-	-	-	U	-	U	-	-	-	U	U	-	-	0,0	0,1	31,6	30,4	16,2	0,0	0,0	0,0	0,0	0,2	0,0	0,0
29743	C	-	-	-	-	-	-	-	-	-	-	-	U	-	-	0,1	0,0	0,0	0,0	32,1	0,0	0,0	0,1	0,0	13,5	0,1	0,1

106

SUPPLEMENTARY TABLES

Supplementary Table S1. List of GISAID identifiers for sequences used in the present study.

All genomes analyzed here were obtained in our laboratory (University hospital institute Méditerranée Infection, Marseille, France). The GISAID sequence database is accessible at: (https://www.gisaid.org/) [3].

Source sample	GISAID identifier
Respiratory samples	
	EPI_ISL_10816729
	EPI_ISL_10816731
	EPI_ISL_10816733
	EPI_ISL_10816740
	EPI_ISL_10816742
	EPI_ISL_10816743
	EPI_ISL_10816744
	EPI_ISL_11030507
	EPI_ISL_2757096
	EPI_ISL_3054898
	EPI_ISL_3054899
	EPI_ISL_3055037
	EPI_ISL_3055223
	EPI_ISL_3055225
	EPI_ISL_3055227
	EPI_ISL_3055234
	EPI_ISL_3055235
	EPI_ISL_3830105
	EPI_ISL_3830215
	EPI_ISL_3831874
	EPI_ISL_3933559
	EPI_ISL_3933565
	EPI_ISL_3933569
	EPI_ISL_3933571
	EPI_ISL_3933572
	EPI_ISL_3934656
	EPI_ISL_3934682
	EPI_ISL_3934683
	EPI_ISL_4394365

Supplementary Table S1 - continued

	EPI_ISL_4944362
	EPI_ISL_4944364
	EPI_ISL_4951784
	EPI_ISL_4951785
	EPI_ISL_6332079
	EPI_ISL_6737742
	EPI_ISL_7376142
	EPI_ISL_7376355
	EPI_ISL_8321213
	EPI_ISL_8321223
	EPI_ISL_8321228
	EPI_ISL_8321229
	EPI_ISL_8321241
	EPI_ISL_8321242
	EPI_ISL_8321256
	EPI_ISL_8709907
	EPI_ISL_8709910
	EPI_ISL_8711731
	EPI_ISL_9773781
	EPI_ISL_9774389
	EPI_ISL_9774894
	EPI_ISL_9774895
Culture supernatants	
	EPI_ISL_10816730
	EPI_ISL_10816732
	EPI_ISL_10816734
	EPI_ISL_10816735
	EPI_ISL_10816738

References

1. La Scola, B.; Le Bideau, M.; Andreani, J.; et al. Viral RNA load as determined by cell culture as a management tool for discharge of SARS-CoV-2 patients from infectious disease wards. *Eur J Clin Microbiol Infect Dis.* **2020**, *39*, 1059-1061.
2. Colson, P.; Fournier, PE.; Chaudet, H.; et al. Analysis of SARS-CoV-2 Variants From 24,181 Patients Exemplifies the Role of Globalization and Zoonosis in Pandemics. *Front Microbiol.* **2022**, *12*, 786233. doi: 10.3389/fmicb.2021.786233.

3. Alm, E.; Broberg, EK.; Connor, T.; et al. Geographical and temporal distribution of SARS-CoV-2 clades in the WHO European Region, January to June 2020. *Euro Surveill.* **2020**, *25*, 2001410.